Hindawi
Advances in Condensed Matter Physics
Volume 2020, Article ID 2891790, 7 pages
https://doi.org/10.1155/2020/2891790

Research Article

Generation of (3, 1) Vector Signal Based on Probabilistic Shaping Technology without Precoding

Jiangnan Xiao, Xu Dong, Bo Liu, Xingxing Feng, Chuang Zhao, and Jiangli Zuo

Shanghai Key Lab of Modern Optical Systems,
Terahertz Technology Innovation Research Institute, and Engineering Research Center of Optical Instrument and System, Ministry of Education, University of Shanghai for Science and Technology, Shanghai 200093, China

Correspondence should be addressed to Jiangnan Xiao; jiangnanxiao@usst.edu.cn

Received 10 August 2020; Accepted 25 September 2020; Published 26 October 2020

Academic Editor: Junmin Liu

In this paper, we introduce the probabilistic shaping (PS) technique to the normal (3, 1) vector signal and simulate the generated PS (3, 1) photonic vector signal on an optical transmission system. The PS (3, 1) photonic vector signal is generated by a radio frequency (RF) signal at 12 GHz driving a Mach–Zehnder modulator- (MZM-) based optical carrier suppression (OCS) doubling, and the PS (3, 1) photonic vector signal is not precoding. The PS (3, 1) photonic vector signal and the normal (3, 1) photonic vector signal are used to transmit in 5 km, 10 km, and 20 km single-mode fibers (SMF), respectively. The simulation results demonstrate that the bit error ratio (BER) of the PS (3, 1) vector signal is less than the forward error correction (FEC) threshold of 3.8×10^{-3}, and the BER performance is better than that of the normal (3, 1) vector signal at 4 Gbit/s and 8 Gbit/s transmission rates.

1. Introduction

Optical communication is a communication method using the laser as the carrier and fiber optics as the transmission medium, which has the advantages of huge carrier resources and small transmission attenuation. Internet business has been exploding as people's demand for information expands dramatically, and the bandwidth demand for network data services continues to increase. Now, more and more video streams, as well as cloud computing, and mobile data transmission put forward higher requirements on optical communication system network size, communication speed, communication capacity, and communication distance. The radio-over-fiber (ROF) communication combines optical communication and wireless transmission, which offers the advantages of high bandwidth, low loss, low power consumption, and flexible operation [1–6]. Besides, the vector modulation format has high spectral efficiency and allows more information to be transmitted in a limited bandwidth, thus reducing the bandwidth requirements on optical devices [7]. The transmission capability is effectively increased by the vector modulation in the ROF system, and it is widely used to drive external modulators using low-cost radio frequency (RF) signals, which generate more stable photonic vector signals based on the optical carrier suppression (OCS) technique [3–6].

Since the power limitations are caused by the fiber channel, the signal must be optimized to increase the spectral efficiency and transmission capacity without increasing the transmit power. The probabilistic shaping (PS) technique is an excellent solution to these problems, as its purpose is to decrease the probability of signal positions with high energy and increase the probability of signal positions with low energy, thus reducing the average transmitted energy. As can be seen from recent studies, it can be seen that the PS can provide longer transmission distance, larger transmission capacity, and higher transmission rate [8–16], which has become a hot issue of discussion.

At present, Xiao et al. [17] demonstrate that a (3, 1) vector signal has superior bit error ratio (BER) performance than the quadrature phase shift keying (QPSK) vector signal in the optical transmission. This scheme does not require amplitude precoding, and the data from the (3, 1) vector signal are acquired primarily as phase information. Combined with the square-law property of the photodetector

(PD), the Euclidean distance between the (3, 1) vector signal constellations is balanced, effectively avoiding the phased precoding operations and reducing the complexity of the system. In this paper, the PS technique is invoked to further optimize the system performance, and a (3, 1) photonic vector signal based on the PS technique is generated, hereinafter referred to as the PS (3, 1) photonic vector signal. The PS (3, 1) photonic signal is generated by the PS (3, 1) electronic vector signal as an RF signal at 12 GHz driving an external Mach–Zehnder modulator (MZM). Then, the PS (3, 1) photonic vector signal is simulated by an optical transmission system for transmission in 5 km, 10 km, and 20 km single-mode fibers (SMF), respectively. The simulation results demonstrate that the method has a BER lower than the forward error correction (FEC) threshold of 3.8×10^{-3} in optical transmission at 4 Gbit/s and 8 Gbit/s transmission rates, and the BER performance of the PS (3, 1) vector signal is better than that of the normal (3, 1) vector signal.

2. Principles

2.1. Principle of PS Technique. The PS is a modulation optimization technique that obeys our predefined probabilistic distribution for the probability of each symbol occurring in the signal after coding and mapping. This probabilistic distribution is characterized by an increase in the probability of occurrence of the midzero position constellation point and a decrease in the probability of occurrence of the outer three-position constellation points compared to the normal (3, 1) signal that is uniformly distributed, as shown in Figure 1. As a result, the probability of occurrence of low BER constellation positions is increased and the probability of occurrence of high BER constellation positions is decreased, thus improving the BER performance of the system. Figure 1(a) shows the probability distribution of normal (3, 1) signal constellation positions, and Figure 1(b) shows the probability distribution of PS (3, 1) signal constellation positions, respectively. In addition, the average power of the PS (3, 1) signal will be lower than the average power of the normal (3, 1) signal after decreasing the probability of the occurrence of positions with higher amplitude, thus saving the transmit power and helping to solve the power limitations issue due to the nonlinearity in optical communication.

The probability distribution used in this paper is the Maxwell–Boltzmann distribution as follows:

$$P_X(x_i) = \frac{1}{\sum_{k=1}^{M} e^{-vx_k^2}} \times e^{-vx_i^2}, \tag{1}$$

this is a formula for one-dimensional symbols, which can calculate the probability for each distribution position of the (3, 1) signal, where v is the scaling factor, and its larger value represents a higher level of the PS, and M represents the number of constellation positions. For multiple signals, it can also be written as

$$P_X(x_i) = \frac{1}{\sum_{k=1}^{M} e^{-v\left(\mathrm{Re}(x_i)^2+\mathrm{Im}(x_i)^2\right)}} \times e^{-v\left(\mathrm{Re}(x_i)^2+\mathrm{Im}(x_i)^2\right)}. \tag{2}$$

Here, we first set the value of v to 0.4, and then the probability of the outer three-position constellation points and the midzero position constellation point appearing is 0.222626675641, 0.222626675641, 0.222626675641, and 0.332119973077, respectively. Thus, the achievable information rate (AIR) reaches 1.9756 bit/symbol. By the following power calculation formula,

$$\overline{P} = \sum_i |X_i|^2 \times P(X_i), \tag{3}$$

the average relative power of the PS (3, 1) signal can be found to be 0.6679, whereas the normal (3, 1) signal has an average power of 0.7500, which is 1.1230 times higher than that of the PS (3, 1) signal. It is necessary to set the average power of the two to be equal to increase comparability; therefore, the amplitude of each symbol of the PS (3, 1) signal should be increased by a factor of 1.0587, as shown in Figure 2. Figure 2(a) shows the constellation of the normal (3, 1) signal, and Figure 2(b) shows the constellation of the expanded PS (3, 1) signal.

2.2. Principle of PS (3, 1) Photonic Vector Signal Generation. Figure 3 shows a principle diagram of the OCS-based PS (3, 1) photonic vector signal generation. First, we produce a pseudorandom binary sequence (PRBS) in MATLAB and then let each symbol of the (3, 1) signal be encoded and mapped by PS so that its probability of occurrence obeys our predefined distribution. Afterward, the generated PS (3, 1) signal is divided into I and Q channels and are mixed with two sinusoidal RF signals in the orthogonal phase at f_s, respectively, and then upconverted to the intermediate frequency (IF) signal. Finally, the two signals are superimposed to generate the PS (3, 1) electronic vector signal, as shown in Figure 3(a). The PS (3, 1) electronic vector signal is used as RF, and the PS (3, 1) photonic vector signal is then generated through MZM driven by the RF. Figure 3(b) shows the relationship between MZM output power and direct current (DC) bias voltage. The DC bias voltage of the MZM needs to be set to the minimum transmission point to realize the OCS technique. Then, the two first-order sidebands are generated, and the frequency of the optical carrier becomes $2f_s$. The optical spectrum of the signal at the MZM output is shown in Figure 3(c). PD conversion follows the square law, and Figures 3(d) and 3(e) show the change in constellation points before and after PD, which are mapped point by point with the same color. Upon comparison, it can be seen that the constellation points after PD have changed the phase at "10" and "11," and it is only necessary to change the decoding method to correct this error due to the phase change.

3. The Construction of Simulation System

Figure 4 shows the system simulation platform built to research the PS (3, 1) vector signal. In the transmission system, the PS (3, 1) electronic vector signal is amplified and used as RF to drive the MZM to generate the PS (3, 1) photonic vector signal. The PS (3, 1) electronic vector signal

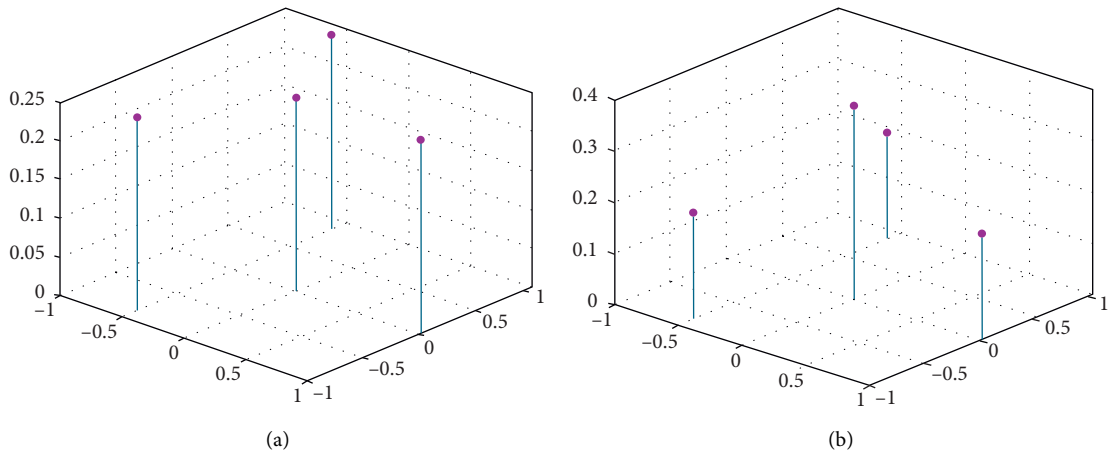

Figure 1: The probability distributions of (a) the normal (3, 1) signal and (b) the PS (3, 1) signal constellation positions.

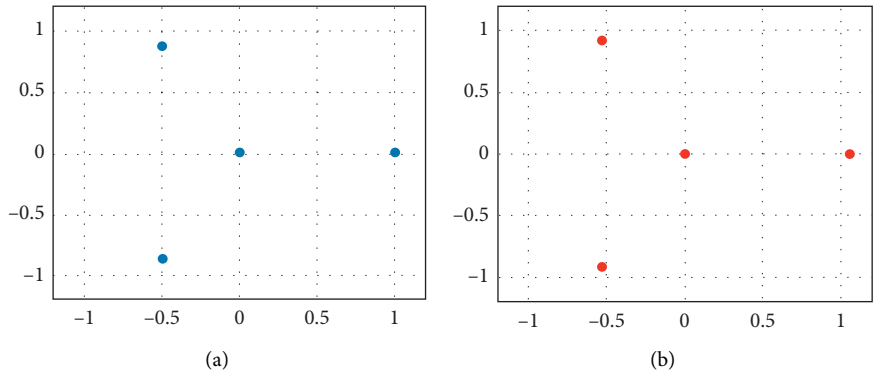

Figure 2: (a) Normal (3, 1) and (b) PS (3, 1) signal constellations.

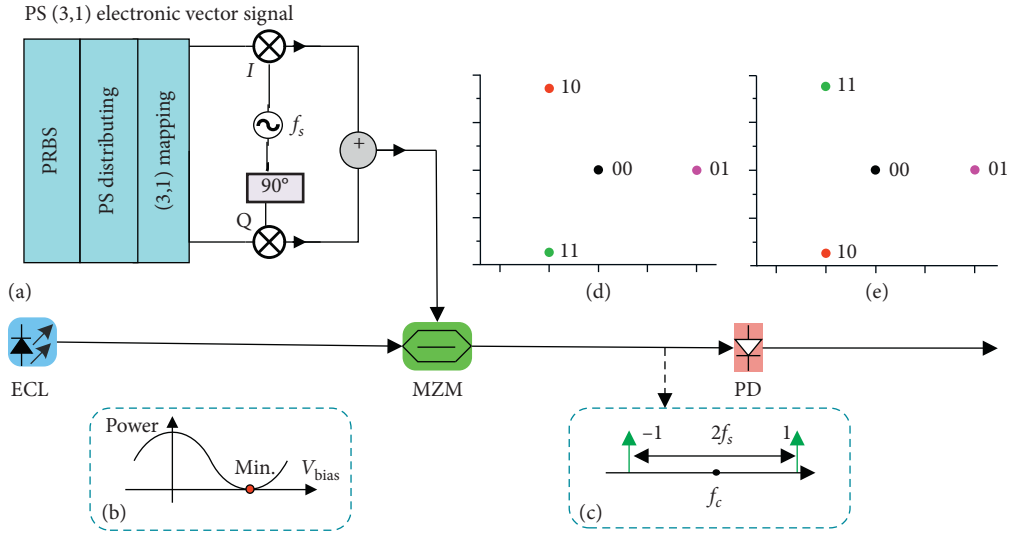

Figure 3: Schematic diagram of PS (3, 1) photonic vector signal generation: (a) the method of generating PS (3, 1) electronic vector signals; (b) relationship between MZM output power and DC bias voltage; (c) optical spectrum of the signal at the MZM output; (d) distribution of pre-PD constellation points; (e) distribution of post-PD constellation points.

is generated at 12 GHz by MATLAB offline programming. The length of PRBS is 2^{14}, and the sampling rate is set to 64 GSa/s. The tunable external cavity laser (ECL) has a transmit center frequency of 191.1 THz, a line width setting of 100 kHz, and an average power setting of 16 dBm. Figure 4(a) shows the spectrogram of the PS (3, 1) photonic

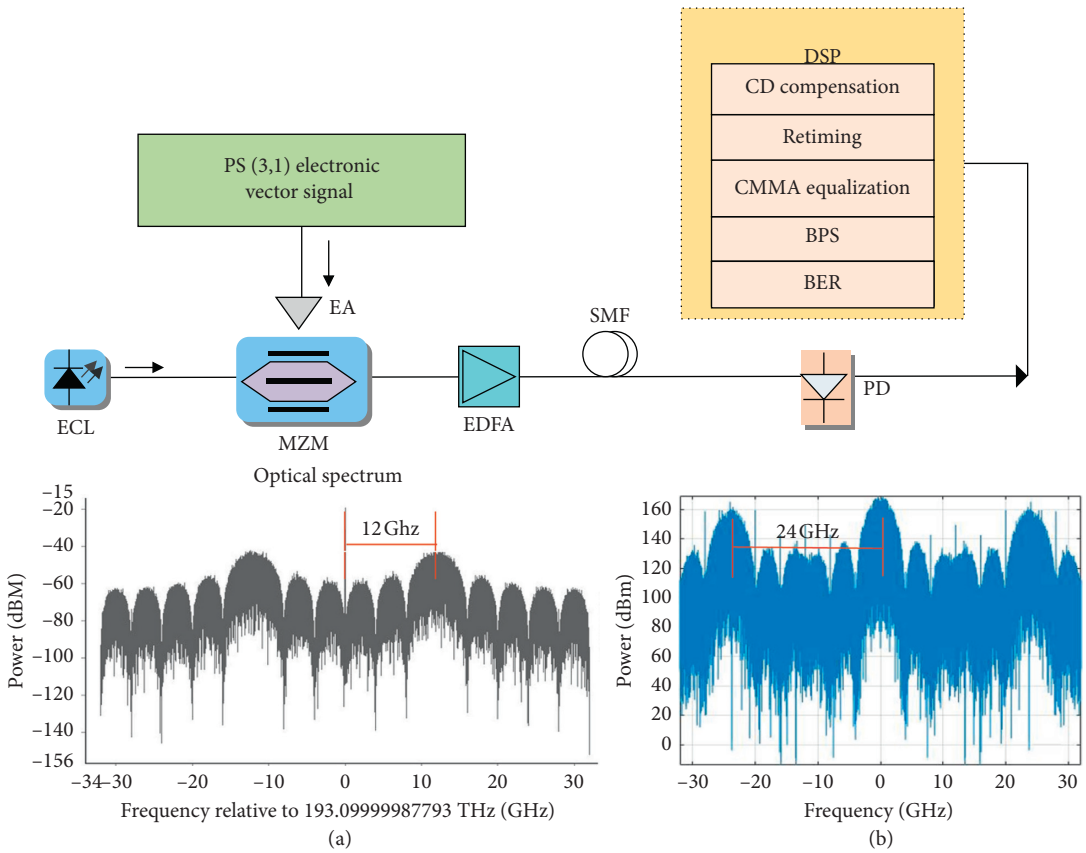

FIGURE 4: PS (3, 1) vector signal system diagram: (a) spectrogram of the PS (3, 1) photonic vector signal with $v = 0.4$ at 12 GHz after MZM; (b) spectrogram of the PS (3, 1) vector signal with $v = 0.4$ after PD.

vector signal with $v = 0.4$ after MZM. The PS (3, 1) photonic vector signal is transmitted through the SMF after an erbium-doped fiber amplifier (EDFA), and the length of SMF is set at 5 km, 10 km, and 20 km. The attenuation coefficient of SMF is 0.2×10^{-3} db/m, the chromatic dispersion at 1550 nm is 16×10^{-6} s/m^2, and the dispersion slope is 0.08×10^3 s/m^3. The PD has a sensitivity of 1 A/W, and Figure 4(b) shows the spectrogram of the PS (3, 1) vector signal with $v = 0.4$ after PD, which is a 24 GHz carrier bandwidth after doubling the frequency. Finally, the binary sequence recovery is done by digital signal processing (DSP), including downconversion, chromatic dispersion (CD) compensation, clock extraction, constant multimodulus algorithm (CMMA), blind phase search (BPS) algorithm, and BER calculation.

Figure 5 shows the constellation of the PS (3, 1) vector signal generated at $v = 1.5$ with a transmission rate of 4 Gbit/s after 5 km SMF in the optical system. These DSP steps include (a) the constellation of the original signal, (b) the constellation after clock extraction, (c) the constellation after CMMA, and (d) the constellation after BPS. The probability of the outer three-position constellation points and the midzero position constellation point appearing is 0.133659657679, 0.133659657679, 0.133659657679, and 0.599021026963, respectively. For a better view of the results, the DSP is shown here when the received optical power is −27 dBm. It is clear from the figure that more of the data are concentrated at the midzero position, which is caused by the PS technique.

4. Simulation Results

We transmit the single carrier normal (3, 1) vector signal and the PS (3, 1) vector signal with $v = 0.4$ over a 5 km SMF at 4–8 Gbaud, respectively. Figure 6 shows the BER versus the baud rate for the two cases when the received optical power is −23 dBm. The PS (3, 1) vector signal at 7 Gbaud already has a BER below the FEC threshold of 3.8×10^{-3}, so the achievable maximum baud rate of the single carrier PS (3, 1) vector signal over a 5 km SMF reaches 7 Gbaud at a received optical power of −23 dBm. The AIR of the PS (3, 1) vector signal is 1.9756 bit/symbol, so here the maximum bit rate that the PS (3, 1) vector signal can achieve is $7 \times 1.9756 = 13.8292$ Gbit/s. For the same baud rate of 7 Gbaud, the BER of the normal (3, 1) vector signal is higher than 3.8×10^{-3}, which is below the FEC threshold at 6 Gbaud. Thus, the achievable maximum baud rate of the normal (3, 1) vector signal with the AIR of 2 bit/symbol is 6 Gbaud at a received optical power of −23 dBm. The maximum bit rate that the normal (3, 1) vector signal can achieve is $6 \times 2 = 12$ Gbit/s, which is smaller than the value of the PS (3, 1) vector signal. The simulation result demonstrates that the BER of the PS (3, 1) signal is much better than that of the normal (3, 1) signal at 4–8 Gbaud, which can be summarized as the PS technique is

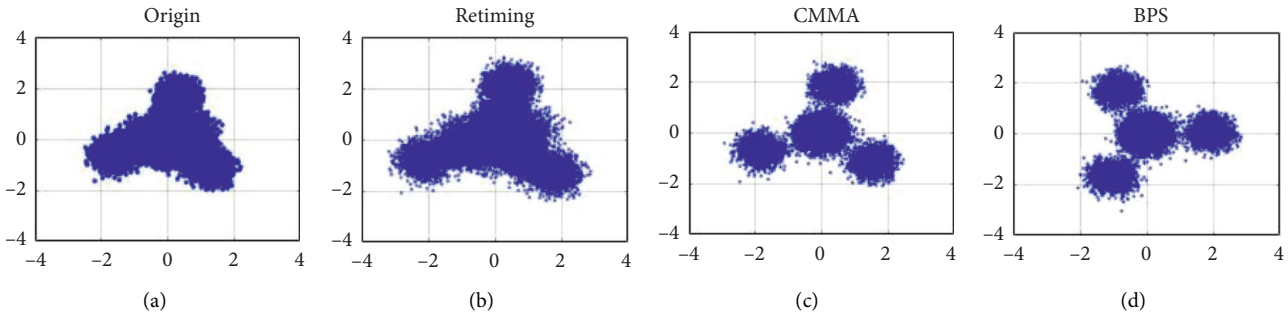

FIGURE 5: Constellation for the 4 Gbit/s over 5 km SMF transmission when the received optical power is −27 dBm: (a) the constellation of the original signal; (b) the constellation after clock extraction; (c) the constellation after CMMA; (d) the constellation after BPS.

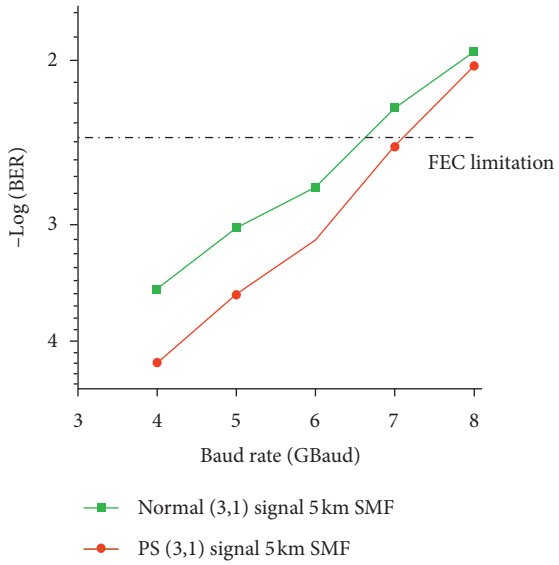

FIGURE 6: BER of the normal (3, 1) vector signal and the PS (3, 1) vector signal with $v = 0.4$ versus baud rate for 5 km SMF transmission at a received optical power of −23 dBm, respectively.

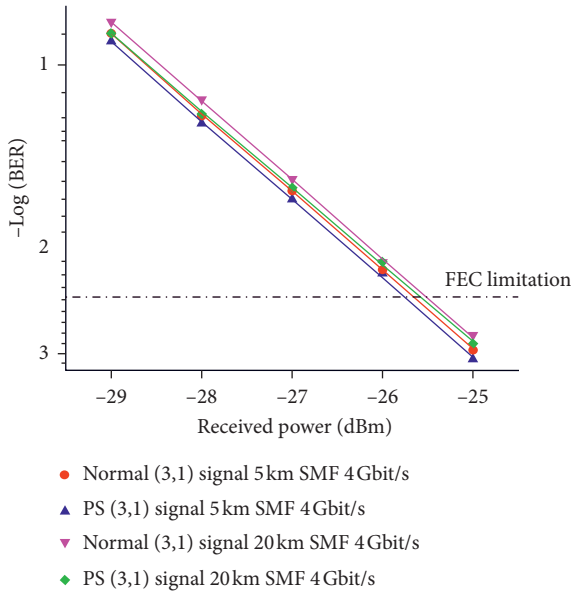

FIGURE 7: BER of the normal (3, 1) signal and the PS (3, 1) signal versus received optical power for 5 km and 20 km SMF transmission at 4 Gbit/s, respectively.

sacrificing a small amount of spectral entropy for a large reward from BER performance. In the following, we further investigate the improvement of the system BER performance by the PS technique.

Considering that the spectral entropy of the PS (3, 1) vector signal will be less than 2 bit/symbol, the same baud rate represents a small deviation from the information rate, so it is necessary to compare the BER performance at the same bit rate. Figures 7 and 8 show the BER of a single carrier normal (3, 1) vector signal and the PS (3, 1) vector signal versus received optical power for 5 km and 20 km SMF transmission at 4 Gbit/s and 8 Gbit/s, respectively. The PS (3, 1) photonic vector signal generated at $v = 0.4$ is used here, and then probability of the outer three-position constellation points and the midzero position constellation point appearing is 0.222626675641, 0.222626675641, 0.222626675641, and 0.332119973077, respectively. Figure 7 shows the BER versus the received optical power for four different cases: (1) normal (3, 1) signal 5 km SMF 4 Gbit/s, (2) PS (3, 1) signal 5 km SMF 4 Gbit/s, (3) normal (3, 1) signal 20 km SMF 4 Gbit/s, and (4) PS (3, 1) signal 20 km SMF 4 Gbit/s. The simulation result demonstrates that the BER of the PS (3, 1) vector signal over the 20 km SMF is less than the FEC threshold of 3.8×10^{-3} when the received optical power is −25 dBm, and the overall BER performance is better than that of the normal (3, 1) vector signal. This result is completely consistent with the theoretical analysis. Figure 8 also shows the BER versus the received optical power for four different cases: (1) normal (3, 1) signal 5 km SMF 8 Gbit/s, (2) PS (3, 1) signal 5 km SMF 8 Gbit/s, (3) normal (3, 1) signal 20 km SMF 8 Gbit/s, and (4) PS (3, 1) signal 20 km SMF 8 Gbit/s. The simulation result demonstrates that the BER of the PS (3, 1) vector signal over the 20 km SMF is less than the FEC threshold of 3.8×10^{-3} when the received optical power is −23 dBm, and the overall BER performance is better than the normal (3, 1) vector signal.

Figure 9 shows the BER of the normal (3, 1) vector signal and the PS (3, 1) vector signal versus received optical power for 5 km, 10 km, and 20 km SMF transmission at 16 Gbit/s, respectively. We also set the PS (3, 1) photonic vector signal generated at $v = 0.4$. The simulation result demonstrates that

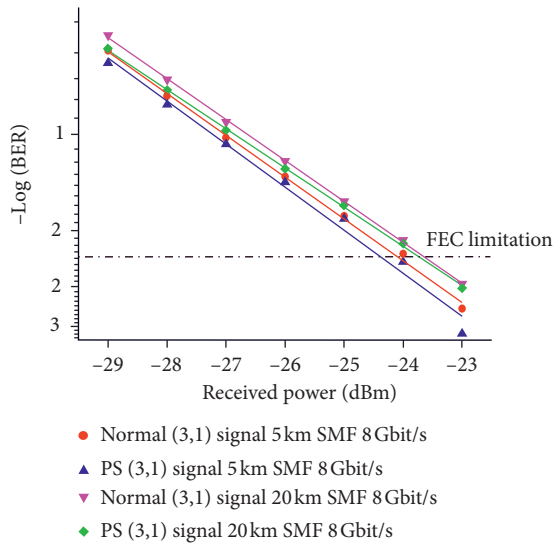

Figure 8: BER of the normal (3, 1) signal and the PS (3, 1) signal versus received optical power for 5 km and 20 km SMF transmission at 8 Gbit/s, respectively.

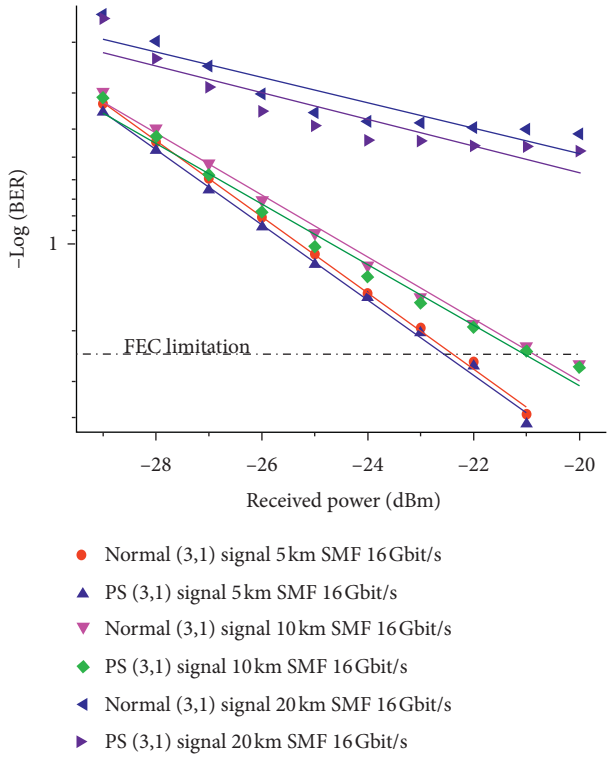

Figure 9: BER of the normal (3, 1) signal and the PS (3, 1) signal versus received optical power for 5 km, 10 km, and 20 km SMF transmission at 16 Gbit/s, respectively.

the BER of the PS (3, 1) vector signal over 5 km SMF is less than the FEC threshold of 3.8×10^{-3} when the received optical power is −22 dBm, and the BER of the PS (3, 1) vector signal over 10 km SMF is less than FEC threshold of 3.8×10^{-3} when the received optical power is −20 dBm. In addition, the simulation result demonstrates that the PS (3, 1) vector signal over 20 km SMF does not reach the FEC threshold of 3.8×10^{-3} at 16 Gbit/s. However, the overall BER performance of the PS (3, 1) vector signal is still better than that of the normal (3, 1) vector signal.

5. Conclusion

In this paper, we introduce the PS technique to the normal (3, 1) vector signal and simulate the generated PS (3, 1) photonic vector signal on an optical system. The simulation results demonstrate that the maximum reliable information rate of the PS (3, 1) vector signal is higher than that of the normal (3, 1) vector signal in our simulation system, and the PS (3, 1) vector signal has better BER performance than the normal (3, 1) vector signal at the same transmission rates of 4 Gbit/s, 8 Gbit/s, and 16 Gbit/s. From the above results, it can be seen that the PS technique balances both spectral efficiency and BER performance, making the effectiveness and reliability of the optical transmission system guaranteed.

Data Availability

All the data used to support the findings of this study are available from the corresponding author upon request.

Conflicts of Interest

The authors declare that they have no conflicts of interest.

Acknowledgments

This work was supported by funding from the National Key Research and Development Program of China Stem Cell and Translational Research (2018YFB1801500); National Natural Science Foundation of China (61675048); Research Project of Key Laboratory for Information Science of Electromagnetic Waves (MOE) (EMW201911).

References

[1] Y. Xu, Z. Zhang, X. Li, J. Xiao, and J. Yu, "Demonstration of 60 Gb/s W-band optical mm-wave signal full-duplex transmission over fiber-wireless-fiber network," *IEEE Communications Letters*, vol. 18, no. 12, pp. 2105–2108, 2014.

[2] X. Wang, J. Yu, Z. Cao, J. Xiao, and L. Chen, "SSBI mitigation at 60 GHz OFDM-ROF system based on optimization of training sequence," *Optics Express*, vol. 19, no. 9, pp. 8839–8846, 2011.

[3] X. Li, J. Zhang, J. Xiao, Z. Zhang, Y. Xu, and J. Yu, "W-band 8QAM vector signal generation by MZM-based photonic frequency octupling," *IEEE Photonics Technology Letters*, vol. 27, no. 12, pp. 1257–1260, 2015.

[4] J. Xiao, X. Li, Y. Xu, Z. Zhang, L. Chen, and J. Yu, "W-band OFDM photonic vector signal generation employing a single Mach-Zehnder modulator and precoding," *Optics Express*, vol. 23, no. 18, pp. 24029–24034, 2015.

[5] L. Zhao, L. Xiong, M. Liao, J. Xia, Y. Pang, and X. Shi, "W-Band 8QAM vector millimeter-wave signal generation based on tripling of frequency without phase pre-coding," *IEEE Access*, vol. 7, pp. 156978–156983, 2019.

[6] X. Li, "Optimization of precoding phase distribution for frequency-multiplication vector signal generation," *IEEE Photonics Journal*, vol. 9, no. 3, p. 1, Article ID 5502207, 2017.

[7] C.-T. Lin, P.-T. Shih, W.-J. Jiang, E.-Z. Wong, J. J. Chen, and S. Chi, "Photonic vector signal generation at microwave/millimeter-wave bands employing an optical frequency quadrupling scheme," *Optics Letters*, vol. 34, no. 14, pp. 2171–2173, 2009.

[8] B. Liu, X. Li, Y. Zhang et al., "Probabilistic shaping for ROF system with heterodyne coherent detection," *APL Photonics*, vol. 2, no. 5, Article ID 056104, 2017.

[9] B., LiuY. Zhang et al., "Performance comparison of PS star-16QAM and PS square-shaped 16QAM (square-16QAM)," *IEEE Photonics Journal*, vol. 9, no. 6, pp. 1–8, Article ID 2760347, 2017.

[10] M. P. Yankov, D. Zibar, K. J. Larsen, L. P. B. Christensen, and S. Forchhammer, "Constellation shaping for fiber-optic channels with QAM and high spectral efficiency," *IEEE Photonics Technology Letters*, vol. 26, no. 23, pp. 2407–2410, 2014.

[11] F. Buchali, G. Bocherer, W. Idler, L. Schmalen, P. Schulte, and F. Steiner, "Experimental demonstration of capacity increase and rate-adaptation by probabilistically shaped 64-QAM," in *Proceedings of the European Conference on Optical Communication (ECOC)*, Brussels, Belgium, December 2015.

[12] C. Pan and F. R. Kschischang, "Probabilistic 16-QAM shaping in WDM systems," *Journal of Lightwave Technology*, vol. 34, no. 18, pp. 4285–4292, 2016.

[13] W. Idler, F. Buchali, and L. Schmalen, "Field demonstration of 1 Tbit/s super-channel network using probabilistically shaped constellations," in *Proceedings of the European Conference on Optical Communication*, Düsseldorf, Germany, September 2016.

[14] T. Fehenberger, A. Alvarado, G. Böcherer, and N. Hanik, "On probabilistic shaping of quadrature amplitude modulation for the nonlinear fiber channel," *Journal of Lightwave Technology*, vol. 34, no. 21, pp. 5063–5073, 2016.

[15] F. Buchali, F. Steiner, G. Böcherer, L. Schmalen, P. Schulte, and W. Idler, "Rate adaptation and reach increase by probabilistically shaped 64-QAM: an experimental demonstration," *Journal of Lightwave Technology*, vol. 34, no. 7, pp. 1599–1609, 2016.

[16] M. Kong and J. Yu, "Performance improvement on a MIMO radio-over-fiber system by probabilistic shaping," *Optics Communications*, vol. 407, pp. 87–91, 2018.

[17] J. Xiao, X. Feng, W. Zhou et al., "Generation of (3, 1) vector signals based on optical carrier suppression without precoding," *Optics Letters*, vol. 45, no. 4, 2020.